Journal of Applied Mechanics and Technical Physics, Vol. 45, No. 5, pp. 705–711, 2004

INTENSIFICATION OF HEAT TRANSFER IN A DOWNWARD LIQUID-FILM FLOW

E. A. Chinnov, I. A. Sharina, and O. A. Kabov

UDC 536.423.4

Heat transfer in a film flow of the FC-72 *dielectric liquid down a vertical surface with an embedded* 150×150 mm *heater is experimentally examined in the range of Reynolds numbers* $\mathrm{Re} = 5$–375. *A chart of liquid-film flow modes is constructed, and characteristic heat-transfer regions are identified. Data on the dependence of heater-wall temperature and local heat flux at the axis of symmetry of the heater on the longitudinal coordinate are obtained. Local and mean heat-transfer coefficients are calculated. It is shown that enhanced heat transfer is observed in the region where rivulets starts forming in the low-Reynolds-number liquid-film flow.*

Key words: *liquid film, heat transfer, intensification, wave flow, thermocapillary effects.*

INTRODUCTION

The interest in heat-transfer studies of downward liquid-film flows is stipulated by the importance of this process for engineering applications. This topic is discussed in the monographs [1–3]. Generalizing relations and computation algorithms have been proposed [3–5], which normally yield satisfactory results only for moderate heat fluxes and high Reynolds numbers in the film. The majority of reported data were obtained either for extended (longer than 300 mm) heaters [3, 4, 6] or for very short (2.2–6.5 mm) heating elements [7–10]. The influence of three-dimensional deformations of the film surface on heat transfer has not been adequately studied.

Previously, we examined formation of rivulets in the region of two-dimensional and three-dimensional waves in a heated film flow down a vertical surface [11]. It was shown that, in addition to the thermocapillary mechanism resulting in rivulet formation, there exists a thermocapillary wave mechanism.

In the present study, we examine heat transfer in a downward flow of the FC-72 liquid below the saturation temperature past a 150×150 mm heater under conditions of rivulet formation under the action of thermocapillary forces. Since thermocapillary deformations are determined by the temperature gradient on the liquid-film surface, in the present experiments we used a heater designed to ensure redistribution of heat fluxes over the heated surface. The effect of rivulets on heat transfer to the FC-72 liquid flow is analyzed.

1. EXPERIMENTAL RESULTS

Experimental Conditions. The experimental setup and measurement techniques were described in detail in [12]. Specific features of the setup and heater in operation under low Reynolds numbers were discussed in [11].

The heat-transfer study of the low-boiling FC-72 liquid was performed on a shielded test section with a condenser installed in the vapor–gas space. The initial film temperature and the shield temperature were equal to

Kutateladze Institute of Thermophysics, Siberian Division, Russian Academy of Sciences, Novosibirsk 630090; chinnov@itp.nsc.ru. Translated from Prikladnaya Mekhanika i Tekhnicheskaya Fizika, Vol. 45, No. 5, pp. 109–116, September–October, 2004. Original article submitted June 4, 2003; revision submitted October 30, 2003.

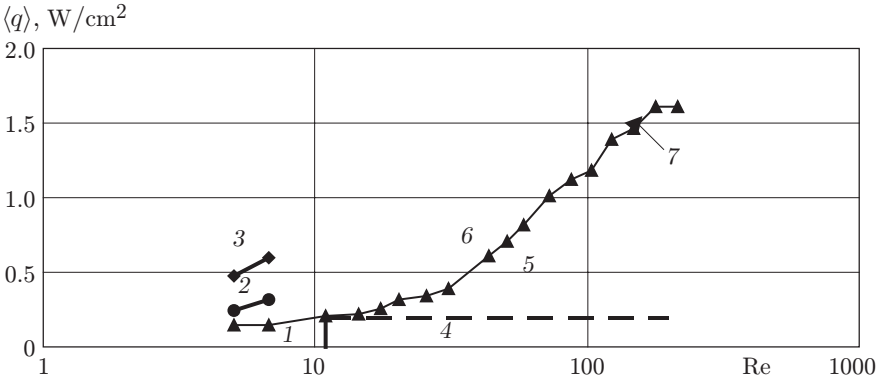

Fig. 1. Chart of flow modes of the FC-72 film flow down the (150 × 150)-mm heater, X_n = 41.5 mm: 1) two-dimensional waves on the film surface; 2) formation of stable structures over part of the heater with dry strips in between; 3) formation of a uniform rivulet flow over the entire heater with evaporation of rivulets in the lower part of the heater; 4) three-dimensional synchronized waves; 5) formation of rivulets; 6) spreading of dry spots between the rivulets; 7) film breakdown.

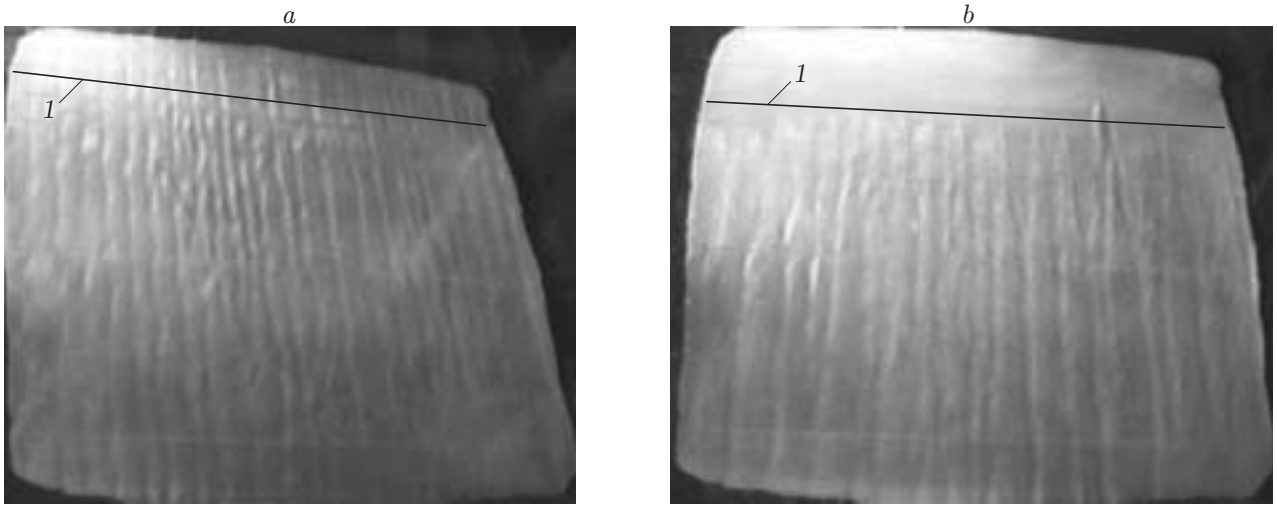

Fig. 2. Photograph of the FC-72 film flow: (a) Re = 51, $\langle q \rangle$ = 0.61 W/cm^2, and L_b = 10.2 mm (line 1); (b) Re = 113.7, $\langle q \rangle$ = 1.19 W/cm^2, and L_b = 30.2 mm (line 1).

the ambient-air temperature, $T_0 = 20°$C. Previous measurements of FC-72 vapor concentration [8] proved that the test-section structure could sustain the equilibrium state of the vapor–gas mixture far from the liquid film at the heater level. No film evaporation occurred without heating. All experiments were carried out under the atmospheric pressure. With increasing heat-flux density and liquid temperature, enhanced evaporation was observed. The temperature of the vapor–gas mixture increased, and the excessive air was displaced from the test chamber through a thin capillary communicating with the atmosphere. The weight concentration and partial pressure of the vapors of the FC-72 liquid increased. The distance X_n between the nozzle of the film-forming device and the upper edge of the heater was 41.5 mm.

Flow Modes and Heat-Transfer Regimes. The hydrodynamics of rivulet formation in a heated downward FC-72 liquid-film flow was described in [11]. Figure 1 shows the chart of flow modes of the FC-72 film flow down the heater. The mean heat-flux density $\langle q \rangle$ was calculated from the power supplied to the heater, and the film Reynolds number was deduced from the dependence $\mathrm{Re} = \Gamma/\mu$, where Γ [kg/(m · sec)] is the specific flow rate of the liquid flow and μ [kg/(m · sec)] is the dynamic viscosity of the liquid. Figure 2 shows the photographs of the film flow; the place where the thermal boundary layer of the liquid reaches the film surface is marked as line 1. In

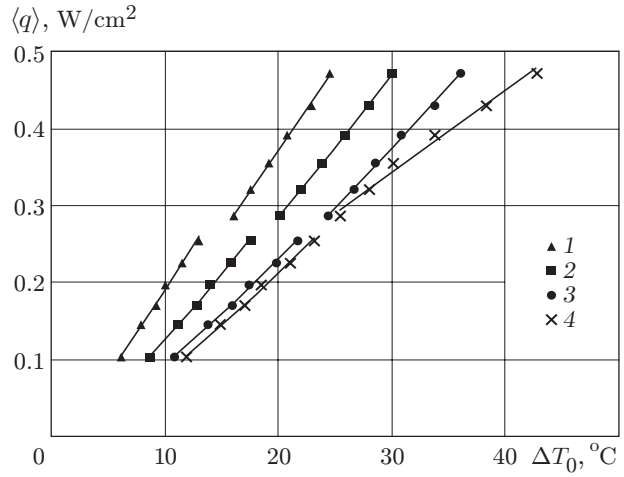

Fig. 3. Mean heat-flux density $\langle q \rangle$ versus the temperature difference ΔT_0 for $\mathrm{Re} = 5$ and $X_t = 2.25$ (1), 20.3 (2), 80.2 (3), and 143.95 (4) mm.

the laminar flow, the length of the initial section ending at the point where the heated layer reaches the film surface can be found from the following formula (see [3]):

$$L_b = 0.139 l_\nu \mathrm{Pr}\, \mathrm{Re}^{4/3}\,. \tag{1}$$

Here $l_\nu = (\nu^2/g)^{1/3}$ (ν is the kinematic viscosity and g is the acceleration of gravity) and Pr is the Prandtl number. The regions of a continuous liquid-film flow with two-dimensional waves on the film surface in the upper part of the heater and an indistinctly pronounced three-dimensional flow pattern in the middle part of the heater, respectively (region 1), and also the region of three-dimensional synchronized waves descending from the upper part of the heater (region 4) are indicated in Fig. 1. These flow modes, separated from each other by the line $\mathrm{Re} = 11$, were observed with heat-flux densities $\langle q \rangle < 0.2$ W/cm^2. The region where rivulets of type B (see [11]) emerge on the crests of synchronized waves on the surface of the continuous liquid film (region 5) is also shown. The rivulets are registered for heat-flux densities $\langle q \rangle > 0.2$ W/cm^2 until stationary dry spots emerge (curve 7). In region 6 of development of rivulet flows and spreading of dry spots between them, formation lines of stable structures (segment 2) and a uniform rivulet flow over the entire heater with partial evaporation of the rivulets in the lower part of the heater (segment 3) are identified. These flow modes for the FC-72 liquid films were observed only at low Reynolds numbers.

Figure 3 shows the experimental dependences of the mean heat-flux density $\langle q \rangle$ versus the temperature difference $\Delta T_0 = T_w - T_0$ in the FC-72 liquid flow past the heater. For $X_t = 2.25$ mm (X_t is the distance between the upper edge of the heater plate and the thermocouple), the dependence $\langle q \rangle$ displays an inflection, which indicates that the heat-transfer law changes as the heat-flux density increases. The change in heat-transfer mechanisms is accompanied by emergence of regular structures of type A [11] with complete evaporation of the film between the rivulets in the region of measurement of the temperature T_w on the heater surface. For $X_t \geqslant 20.3$ mm, the change in heat-transfer modes is not exhibited distinctly. The power exponent in the dependence $\langle q \rangle = \Delta T_0^n$ ($n = 1.2$) displays no substantial changes. The stable rectilinear rivulet flow is violated in this region as the heat fluxes grow in magnitude. The flows become zigzagging, resulting in enhanced wetting of the heater. In the case of rivulet flows ($X_t = 144$ mm), the power exponent n decreases ($n = 0.9$). The most intense evaporation of the liquid, up to complete drying of part of the surface under maximum heat fluxes, is observed in the lower part of the heater. Such heat-transfer regimes were also observed for $\mathrm{Re} = 6.9$. For higher Reynolds numbers, measurements were performed until stable dry spots emerged on the heater surface. Below, we analyze heat transfer to the continuous liquid film until the film breaks down.

Distribution of Temperatures and Heat Fluxes over the Heater Surface. Figure 4 shows the distributions of temperature and dimensionless local heat-flux density $q/\langle q \rangle$ along the heater surface. The local heat-flux density q was calculated from the temperature difference over the steel plate of the heater. For $\mathrm{Re} = 5$

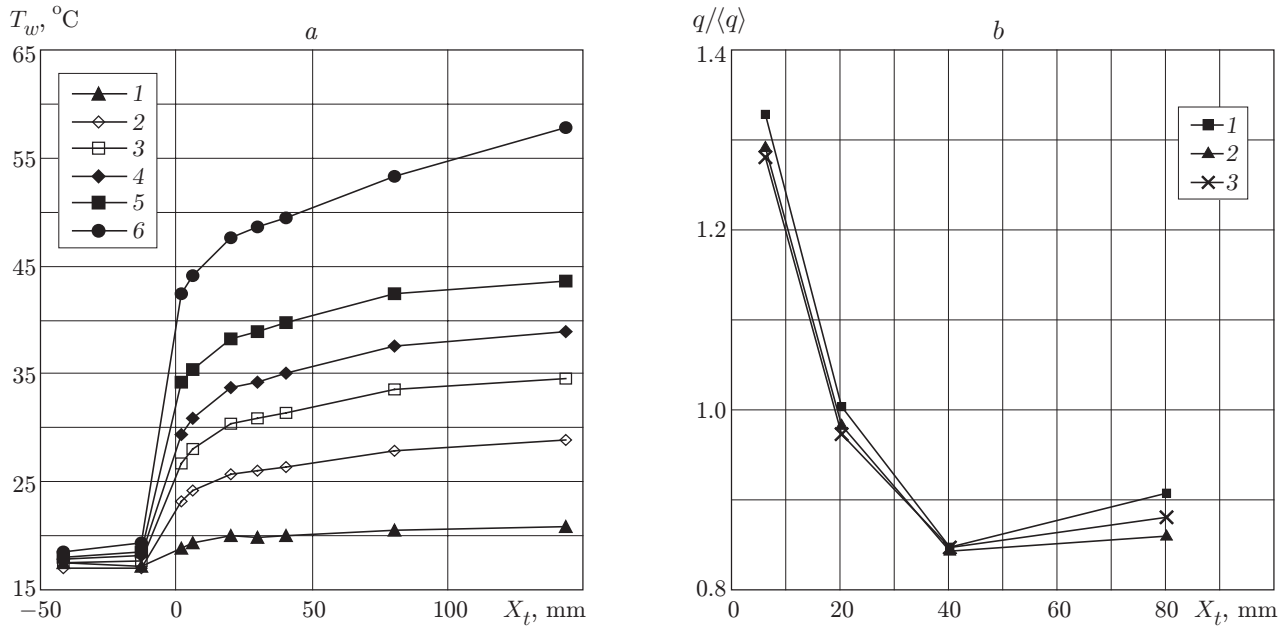

Fig. 4. Distributions of temperature (a) and dimensionless heat-flux density (b) along the heater: (a) Re = 5 and $\langle q\rangle$ = 0.04 (1), 0.1 (2), 0.17 (3), 0.22 (4), 0.29 (5), and 0.43 W/cm^2 (6); (b) Re = 375.7 and $\langle q\rangle$ = 1.19 (1), 1.54 (2), and 1.85 W/cm^2 (3).

and $\langle q\rangle$ = 0.43 W/cm^2, the liquid in the lower part of the heater undergoes evaporation, and the temperature increases linearly with increasing distance X_t. The surface temperature at the lower point of the heater is greater than the boiling point of the FC-72 liquid under normal pressure. For $\langle q\rangle < 0.29$ W/cm^2, the temperature in the lower part of the heater remains almost constant before film breakdown. As was noted in [11], such a nonlinear distribution of temperature is a consequence of the redistribution of the heat flux in the heater; this redistribution depends, apart from the film Reynolds number and the heat flux, on the heat capacity and thermal conductivity of the liquid. An appreciable nonuniformity of heat-flux density along the heater is also observed at high Re (Fig. 4b). For a continuous film flow of the FC-72 liquid, the following relations are valid in the examined range of Reynolds numbers: $0.2 < (q - \langle q\rangle)/\langle q\rangle < 1.4$ and $0.2 < (T_{\max} - T_{\min})/T_{\max} < 0.5$ ($T_{\max}$ and $T_{\min}$ are the maximum and minimum temperatures measured at the heater surface). The temperature distribution along the heater is consistent with the condition $T_w = \text{const}$ rather than with the condition $q = \text{const}$.

2. ANALYSIS OF HEAT TRANSFER

In the majority of previous studies, the heat-transfer coefficient ($\alpha_F = q/\Delta T_F$) was calculated from the difference between the heater-wall temperature and the mean-mass temperature of the film $\Delta T_F = T_w - T_F$. Assuming that the heat-flux density is constant, we calculated the mean-mass temperature of the film by a simple formula [3]. If the condition $q = \text{const}$ is not satisfied (Fig. 4b), the mean-mass temperature of the film can be calculated from the energy-balance relation

$$T_F^* = T_0 + \frac{1}{c_p \mu_0 \operatorname{Re}_0} \int_0^{X_t} [q(x) - q_s(x)]\, dx, \tag{2}$$

where q_s is the density of the heat flux due to evaporation, c_p is the specific heat of the liquid, and μ_0 is the dynamic viscosity; the subscript 0 implies that the value was calculated on the basis of T_0.

Four-point measurements of local heat-flux density on the heater surface (see Fig. 4b), however, do not allow sufficiently accurate approximation of the dependence $q(x)$ along the entire heated surface. The distribution of the

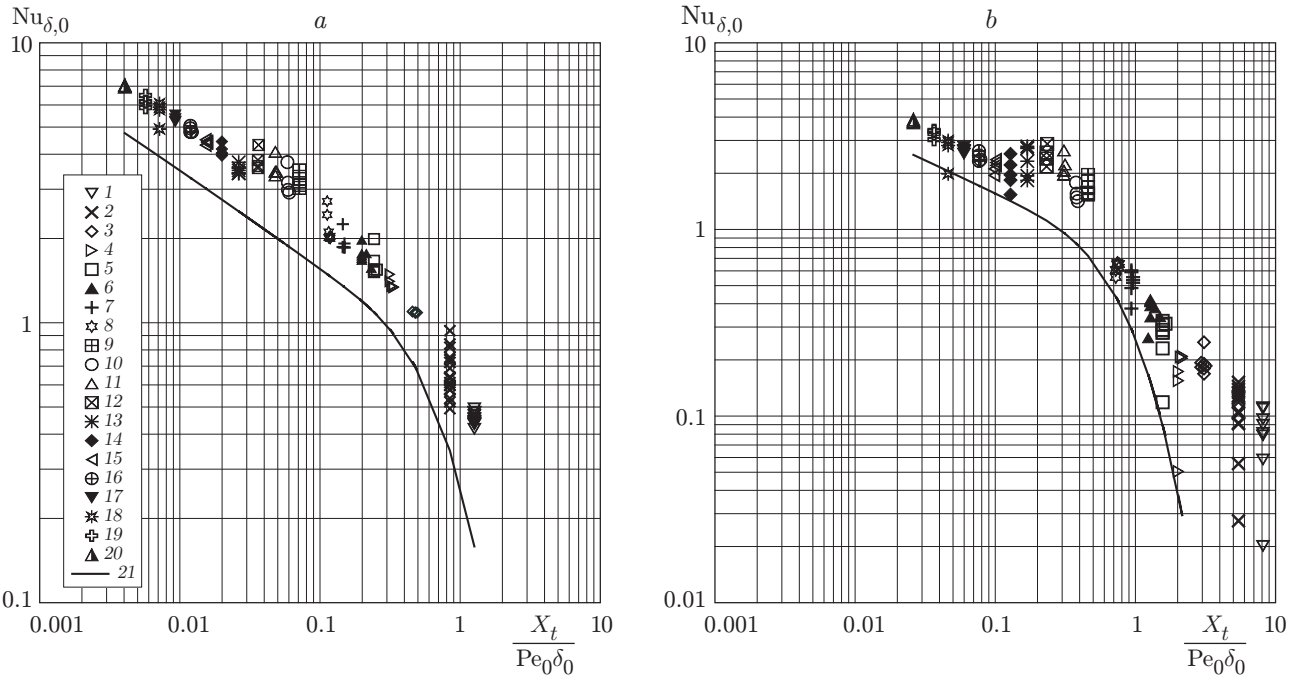

Fig. 5. Nusselt number ($\mathrm{Nu}_{\delta,0} = \alpha_0\delta_0/\lambda_0$) versus $X_t/(\mathrm{Pe}_0\,\delta_0)$ for Re = 5 (1), 6.85 (2), 10.5 (3), 14.3 (4), 17.4 (5), 20.3 (6), 25.6 (7), 31 (8), 43.7 (9), 51 (10), 58.8 (11), 72.8 (12), 92.3 (13), 113.7 (14), 136.2 (15), 167.6 (16), 201.7 (17), 244.9 (18), 291.3 (19), and 375.7 (20); curve 21 refer to the dependence (3); $X_t = 6.25$ (a) and 40.3 mm (b).

heat-flux density $q_s(x)$ over the film surface is unknown. That is why the experimental data were analyzed in terms of the conventionally local heat-transfer coefficient ($\alpha_0 = q/\Delta T$) calculated on the basis of the local heat-flux density and the difference between the heater-surface temperature (at the measurement point) and the initial temperature of the film ($\Delta T = T_w - T_0$), and also in terms of the mean heat-transfer coefficient ($\langle\alpha\rangle = \langle q\rangle/\Delta T$) calculated on the basis of the mean heat-flux density and the difference between the temperature at the lower measurement point ($X_t = 144$ mm) on the heater and the initial temperature of the film.

Figure 5 shows the Nusselt number ($\mathrm{Nu}_{\delta,0} = \alpha_0\delta_0/\lambda_0$) versus the ratio $X_t/(\mathrm{Pe}_0\,\delta_0)$ (δ_0 is the film thickness). The Peclet number $\mathrm{Pe}_0 = \mathrm{Re}_0\,\mathrm{Pr}_0$ was calculated from the flow rate and physicochemical properties of the liquid at the temperature T_0. The experimental data are compared with the dependence predicted for a planar film flow with $T_w = \mathrm{const}$ (see [13]):

$$\mathrm{Nu}_{\delta,0} = 2\sum_{n=0}^{\infty} B_n \exp\Big(-\frac{8}{12}\,\varepsilon_n^2\,\frac{1}{\mathrm{Pe}_0}\,\frac{X_t}{\delta_0}\Big). \tag{3}$$

Here $B_n = -(1/2)A_n(d\psi_n/dY)_{Y=1}$; A_n, ε_n, and ψ_n are constants and eigenvalues in the heat-transfer problem with $T_w = \mathrm{const}$ under consideration. The well-known analogy between the film flow and the plane-channel flow was used here [3].

It is seen from Fig. 5 that the experimental points lie above the curve calculated by formula (3). The deviation depends on the Reynolds number. Three regions can be identified. For high Reynolds numbers (Re > 70), a smooth film flows past the heater at the measurement points (see Fig. 2b). For all values of X_t in this region, the experimental values differ from the curve predicted by formula (3) by 20–30%. For Re = 30–70, the initial heat-transfer region is indistinctly pronounced (Fig. 2a). In the heater region, upward rivulets are formed on developed synchronized three-dimensional waves. A similar mechanism of rivulet formation was described in [11]. For all values of X_t in the examined range of Reynolds numbers, the experimental points deviate upward from the curve calculated by formula (3) (by 30–55%). Probably, the formation of three-dimensional waves and their further separation into rivulets are processes inherent in heat-transfer intensification. For low Reynolds numbers (Re < 14), two- and three-dimensional waves are observed at the film surface; yet, surface deformations are small in this case.

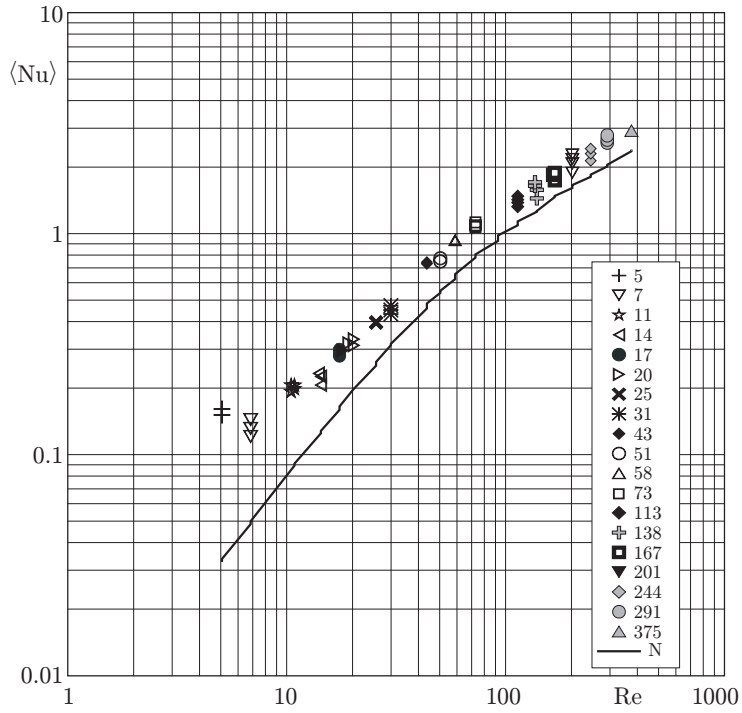

Fig. 6. Nusselt number $\langle \mathrm{Nu} \rangle = \langle \alpha \rangle \delta_0 / \lambda_0$ versus the Reynolds number Re (indicated by numerals), N is the dependence calculated by Eqs. (4) and (5).

A considerable scatter of experimental points in this region results from the effect of variation of heat-flux density. For $X_t = 6.25$ mm, the difference between the mean values is 30% are greater. For larger values of X_t, the difference notably increases, apparently, because of the influence of evaporation, which becomes more pronounced in the lower part of the heater, since a good correlation is observed with the increase in film temperature as a function of q and X_t.

Figure 6 shows a comparison of the experimental mean values of $\langle \mathrm{Nu} \rangle = \langle \alpha \rangle \delta_0 / \lambda_0$ with the theoretical dependence of the Nusselt number (see [1])

$$\alpha_F = 0.0236 \frac{\mu c_p}{L} 4\,\mathrm{Re}_F + 2.07\lambda \left(\frac{g}{\nu^2} \right)^{1/3} (4\,\mathrm{Re}_F)^{-1/3}. \tag{4}$$

Here, λ is the thermal conductivity of the liquid and L is the length of the plate. The mean heat-transfer coefficient was calculated using the formula

$$\langle \alpha \rangle = \frac{\alpha_F}{1 + \alpha_F L / (\mu c_p \,\mathrm{Re}_F)}. \tag{5}$$

The experimental data deviate upward from the curve predicted by formulas (4) and (5). For $\mathrm{Re} > 20$, the difference reaches 25–35%. For $\mathrm{Re} < 20$, the disagreement with the theory is fourfold because of the influence of evaporation, which becomes more pronounced as the Reynolds number decreases.

The results obtained in the present study can be summarized as follows. A chart of flow modes for the FC-72 film flow down a (150×150)-mm heater has been constructed. A specific feature is the formation of regular rivulet structures emerging under the action of thermocapillary forces in the heated liquid-film flow in the region of two- and three-dimensional waves. Characteristic regions of heat transfer to the continuous liquid film and to the rivulet flow have been identified. The distribution of temperatures and heat fluxes along the heater have been measured. The local heat-transfer coefficient has been found to increase in the region of stabilized heat-transfer owing to formation of rivulets. Substantial heat-transfer intensification determined by the mean heat-transfer coefficient is observed at low Reynolds numbers under intense evaporation of the liquid film.

This work was supported by the Russian Foundation for Basic Research (Grant No. 02-02-16478).

REFERENCES

1. E. G. Vorontsov and Yu. M. Tananaiko, *Heat Transfer to Liquid Films* [in Russian], Tekhnika, Kiev (1972).
2. B. G. Ganchev, *Cooling of Elements of Nuclear Reactors by Falling Films* [in Russian], Énergoatomizdat, Moscow (1987).
3. G. Gimbutis, *Heat Transfer in Gravity-Induced Liquid-Film Flows* [in Russian], Mokslas, Vil'nyus (1988).
4. W. Wilke, "Warmeubergang an Rieselfilme," *VDI-Forschungsheft H*, No. 490, 1–36 (1962).
5. B. I. Nigmatulin, M. Z. Goryunova, and Yu. V. Vasil'ev, "Generalization of experimental heat-transfer data for liquid film flows over solid surfaces," *Teplofiz. Vys. Temp.*, **19**, No. 5, 991–1001 (1981).
6. T. Fujita and T. Ueda, "Heat transfer to falling liquid films and film breakdown-I (subcooled liquid films)," *Int. J. Heat Mass Transfer*, **21**, 97–108 (1978).
7. O. A. Kabov, "Heat transfer from a heater with a small linear dimension to a freely flowing liquid film," in: *Proc. of the First National Conf. on Heat Transfer* (Moscow, November 21–25, 1994), Vol. 6, Moscow Inst. of Power Eng., Moscow (1994), pp. 90–95.
8. E. A. Chinnov, O. A. Kabov, A. V. Muzykantov, and D. V. Zaitsev, "Influence of plate inclination on heat transfer and breakdown of locally heated flowing liquid film," *Int. J. Heat Technol.*, **19**, No. 1, 31–44 (2001).
9. O. A. Kabov and E. A. Chinnov, "Heat transfer from a local heat source to an underheated liquid film," *Teplofiz. Vys. Temp.*, **39**, No. 5, 758–768 (2001).
10. O. A. Kabov, B. Scheid, I. A. Sharina, and J.-C. Legros, "Heat transfer and formation of rivulet structures in a falling, locally heated thin liquid film," *Int. J. Therm. Sci.*, **41**, 664–672 (2002).
11. E. A. Chinnov and O. A. Kabov, "Jet formation in gravitational flow of a heated wavy liquid film," *Appl. Mech. Tech. Phys.*, **44**, No. 5, 708–715 (2003).
12. E. A. Chinnov, O. A. Kabov, I. V. Marchuk, and D. V. Zaitsev, "Effect of nonlinear thermocapillary deformations on heat transfer and breakdown of falling liquid films," in: *Proc. of the 12th Int. Heat-Transfer Conf.* (Grenoble, August 18–23, 2002), Vol. 2, Elsevier SAS, Grenoble (2002), pp. 495–500.
13. B. S. Petukhov, *Heat Transfer and Resistance of Laminar Liquid Flows through Pipes* [in Russian], Énergiya, Moscow (1967).